Proceedings of the
Annual Stability Conference
Structural Stability Research Council
Pittsburgh, Pennsylvania, May 10-14, 2011

Elastic-plastic Behavior of Semi-Compact Steel Cross-Sections

N. Boissonnade[1], J.P. Jaspart[2], M. Kettler[3], A. Lechner[3]

Abstract
This paper details new design rules for semi-compact sections that are capable of capturing their characteristic elastic-plastic behavior. The formulae have been validated against experimental test results and hundreds of FEM-shell numerical results, on both H-shaped and hollow sections. They offer full continuities between cross-section classes and with all other design formulae of the code, for both sections and members.

1. Introduction – Research objectives and methodology

Present paper focuses on the behavior of so-called semi-compact sections and members, i.e. profiles with plate slenderness (width to thickness ratios) in a certain medium range; they are denoted as Class 3 sections in European standard Eurocode 3 (CEN 2005).
In daily practice, given the European structural shapes production together with the usual S235 and S355 steel grades, few profiles fall within the Class 3 range[4], and most of them can be classified as Class 1 or 2 (compact sections). However, when axial compression becomes significant and/or with increasing use of high strength steels, many profiles come into the semi-compact range, or even within the Class 4 field.
According to Eurocode 3, such Class 3 members must be designed following elastic principles. This result in a sudden drop of resistance between plastic and elastic capacities, as Fig. 1 shows. For example, in the simple situation of mono-axial bending, a 15% jump of resistance between $M_{el,y,Rd}$ and $M_{pl,yRd}$ (strong axis bending resistance) is observed, while a 50% step can be highlighted for weak axis bending between $M_{el,z,Rd}$ and $M_{pl,z,Rd}$; this gap reaches 65% for biaxial bending, and even more for biaxial bending and compression cases.
Obviously, this jump of resistance does not represent accurately the real behavior, has no clear physical meaning, and should then be avoided. Further, several research works (Lechner 2005 and Kettler 2008) show that a non-negligible amount of plastic resistance exists within the Class 3 field, and even indicate that Class 4 cross-sections (slender) may also exhibit a partly-plastic behavior under specific circumstances.

---

[1] Professor, College of Engineering and Architecture of Fribourg, <nicolas.boissonnade@hefr.ch>
[2] Professor, University of Liège, <jean-pierre.jaspart@ulg.ac.be>
[3] PhD, Graz University of Technology, <kettler@tugraz.at> <lechner@tugraz.at>
[4] It is to remembered, though, that classification depends on the distribution of stresses, i.e. on the actual loading of the section

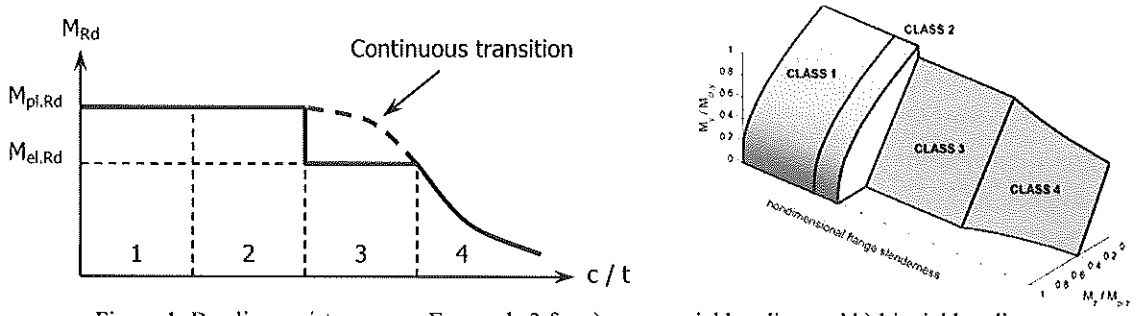

Figure 1: Bending resistance acc. Eurocode 3 for a) mono-axial bending and b) biaxial bending

Hence, present research investigations aim at filling this gap of knowledge; in this respect, a research project named "Semi-Comp" involving several European partners was initiated (Technical University of Graz, University of Liège, F + W GmbH Aachen). The purpose was to provide simple design rules that allow for (i) continuous transitions within the Class 3 field and (ii) a more accurate determination of the real capacity of semi-compact profiles. One of the important objectives of the project was that the design set of formulae had to be in line with Eurocode 3 other rules and principles, so that to be potentially incorporated in the code in a coming version[5]; this implies that the boundaries at the Class 2-3 and Class 3-4 borders have been accepted as such, which is disputable (cf. Boissonnade 2008).
Accordingly, the following methodology was adopted within the "Semi-Comp" project, for both H-shaped and hollow section members:

- Experimental testing, to (i) provide information on semi-compact cross-section and member behavior, and (ii) serve as a reference basis for the validation and assessment of FEM models;
- Development and validation of FEM models against experimental tests. These models should provide sets of reference results through parametric studies ("numerical" tests);
- Development or improvement of design models specific to semi-compact sections and members that aim at taking the benefits of intermediate elastic-plastic behavior;
- Perform additional FEM parametric studies towards safety evaluations where all parameters (dimensions, yield stress...) are defined according to a Monte-Carlo procedure, the aim being the determination of a γ_M safety factor to be associated with the developed models; this last aspect will not be further depicted within present paper, see the project final report for more details (Semi-Comp 2007).

This nowadays "classical" approach is further detailed in the next paragraphs: § 2 presents the test procedures and results for *cross-section* resistance, while § 3 deals with *member* resistance.

2. Cross-section resistance

2.1 Experimental tests

The cross-sectional behavior of semi-compact sections has first been investigated by means of a series of 47 tests at the Technical University of Graz, on different cross-sectional shapes:

- HEAA260, S235 (hot-rolled);

[5] One should perhaps mention that several design codes already propose a different treatment of semi-compact sections: AISC LRFD, BS5950, AS4100...

- HEAA260, S355 (hot-rolled);
- HEAA260, S235 (welded);
- SHS180/180/5, S355 (cold-formed);
- RHS200/120/4, S275 (cold-formed).

All of these five cross-sections and associated steel grades have been selected for all specimens to remain nominally classified as Class 3. The length of the specimen was chosen so that the members were sufficiently short to prevent member buckling, but long enough to exhibit local buckling without significant disturbances from the supports; Table 1 reports information on the different geometrical data used within the tests.

Table 1: Results of tests and FEM simulations for *cross-section* resistance

Specimen	*Section*	*L [mm]*	*Eccentricity [mm]*	*Angle α [°]*	P_{test} *[kN]*	P_{FEM} *[kN]*	$\%_{FEM}$ –
sc-A1-2	*HEAA 260 S235*	900	303.6	-0.3	585.2	558.9	4.7
sc-A1-3			301.7	0.3	812.4	846.3	-4.0
sc-A2-1			301.8	9.5	556.9	556.2	0.1
sc-A2-2			298.1	11.0	554.3	551.7	0.5
sc-A3-1			299.9	40.9	404.5	392.6	3.0
sc-A3-2			298.2	39.6	396.6	399.3	-0.7
sc-A4-1			98.9	90.1	826.8	834.4	-0.9
sc-A4-2			97.8	90.4	824.8	841.6	-2.0
sc-A10-2			95.8	89.6	853.4	864.5	-1.3
sc-A7-1	*HEAA 260 S355*	900	299.2	-0.2	809.6	848.0	-4.5
sc-A7-2			298.5	-0.3	772.3	848.0	-8.9
sc-A1-1			300.2	-0.1	768.5	833.0	-7.7
sc-A8-1			298.8	10.5	790.7	834.0	-5.2
sc-A8-2			298.6	11.4	769.9	803.0	-4.1
sc-A9-1			299.4	39.7	559.1	585.0	-4.4
sc-A9-2			299.1	39.8	602.4	575.0	4.8
sc-A10-1			99.3	89.7	1299.7	1290.0	0.8
sc-A10-3			99.4	90.1	1408.6	1334.9	5.5
sc-A22-1	*HEAA 260 Welded S235*	900	298.8	0.1	545.2	547.0	-0.3
sc-A22-2			298.3	0.4	543.7	552.0	-1.5
sc-A23-1			96.5	89.5	826.3	869.0	-4.9
sc-A23-2			97.8	89.9	842.9	864.0	-2.4
sc-A13-1	*SHS 180/180/5 S355*	700	300.2	0.3	227.9	241.0	-5.4
sc-A13-2			299.2	-0.2	245.6	240.0	-2.3
sc-A13-3			300.2	-0.2	230.8	240.0	-3.8
sc-A14-1			300.7	20.1	240.0	237.0	1.3
sc-A14-2			297.5	19.3	226.1	243.0	-7.0
sc-A14-3			299.9	19.1	233.4	241.0	-3.2
sc-A15-1			298.6	43.9	237.6	244.0	-2.6
sc-A15-2			302.1	45.3	237.3	243.0	-2.3
sc-A15-3			299.6	45.7	235.6	241.0	-2.2
sc-A18-1	*RHS 200/120/4 S275*	700	300.5	20.8	139.5	142.0	-1.8
sc-A18-2			298.1	20.2	142.2	144.0	-1.3
sc-A18-3			298.5	20.0	139.5	144.0	-3.1
sc-A19-1			298.5	44.0	110.7	112.0	-1.2
sc-A19-2			302.8	44.6	112.5	110.0	2.3
sc-A19-3			299.3	45.4	110.8	110.0	0.7

All specimens have been loaded by means of an eccentrically-applied compression load in both principal planes, i.e. the most complex biaxial bending and compression $N_{Ed} + M_{y,Ed} + M_{z,Ed}$ situation was investigated. In practice, bending was mono-axial, and the biaxial bending action

was obtained in varying the orientation of the section's principal axes in comparison to the plane of the applied bending (see Fig. 2); Table 1 summarizes the experimental maximum axial loads.

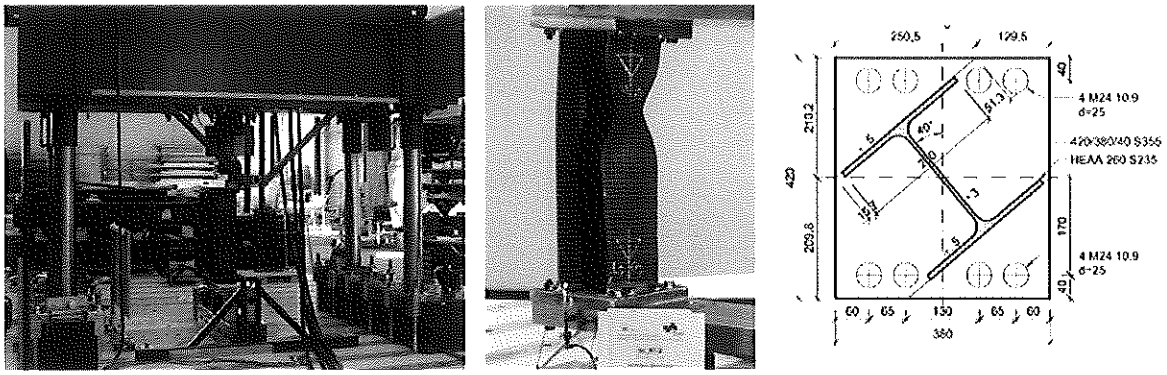

Figure 2: a) General test setup, b) Specimen during test and c) Possible orientation of the section ($\alpha = 40°$)

The experimental investigations were also accompanied by measurements of (i) real σ-ε laws (coupon tests), (ii) local imperfections and (iii) residual stresses, in order to feed the FEM numerical models with the relevant data (see § 2.2).

Since one of the goals of the experimental tests was to quantify the amount of plastic reserve within the Class 3 field (i.e. the influence of the local buckling behavior on the elastic-plastic cross-section capacity), Figs. 3a and 3b propose a specific plotting of the experimental results that help fixing ideas on the potential elastic-plastic resistance reserve.

On the horizontal axis, the non-dimensional slenderness of the governing element (flange or web) of the section is reported, where the Class 3 field is taken as a reference: a section that should be classified at the border between Class 2 and 3 has a non-dimensional slenderness value of 0, while a section that is at the exact limit between Class 3 and four has a slenderness value of 1.0 (see Eq. (2) for exact mathematical definition). On the vertical axis, the "non-dimensional cross-section capacity" is defined as $(R_{exp} - R_{el}) / (R_{pl} - R_{el})$, where an "R-value" represents a load factor leading to "failure" according to *exp*eriments, *pl*astic or *el*astic design. A value equal to 0 then means that the sole elastic resistance may be expected, while a value of 1.0 indicates that the full plastic capacity is available. Such a definition of axes allows for a common plotting of all tests results, which otherwise could not be represented graphically since the loading definition and geometries are different for each test.

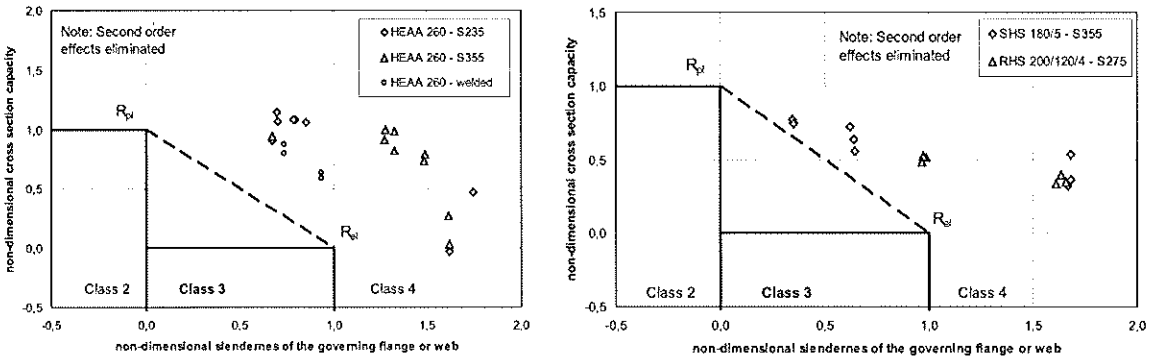

Figure 3: Experimental vs. Eurocode 3 cross-section resistance a) H-shaped sections b) Hollow sections

On the sole light of these experimental results, it is clearly seen that (i) a non-negligible amount of elastic-plastic resistance is available within the Class 3 range, and that (ii) an elastic-plastic behavior could still be accounted for within the Class 4 field, for both H-shaped and hollow sections.

2.2 FEM modeling and parametric studies

As explained before, specific FEM numerical models have been developed, that resort to shell elements: indeed, the key aspect here consists in characterizing the early or late occurrence of local buckling on the behavior of the semi-compact cross-section (thus the need for shell elements). Specific attention has been paid to the meshing of the corner regions and web-to-flange junctions (see Fig. 4), and mesh-density tests have been performed for each possible type of analysis. The possibility to account for both local and global geometrical imperfections has been considered, as well as different distributions of residual stresses. Further details on the validation and development of FEM models are given in dedicated report (Semi-Comp 2007).

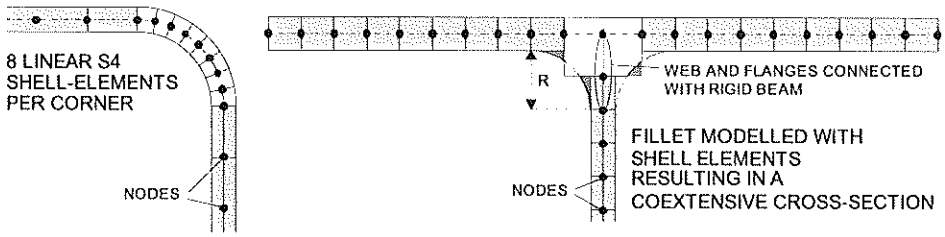

Figure 4: Details on the FE-modeling of the web-to-flange junctions

The FEM models have then been tested against the experimental results. Obviously, all measured data have been introduced in the numerical models, i.e. geometrical dimensions, local imperfections and σ-ε relationships, for the comparison to be as accurate as possible.

The different results are reported in the last columns of Table 1; as can be seen, the numerical results show a very good level of accuracy when compared to the tests (less than 10% difference for each of the 47 tests). By these comparisons, which comprise a lot of different load cases and cross-section slenderness along the Class 3 range, the FE models are seen to be fully satisfactory. Therefore, they have been extensively used in parametric studies to achieve "numerical" tests that should serve as reference results, see § 2.3; a total of 729 FEM-shell GMNIA (Geometrically and Materially Non-linear with Imperfections Analysis) calculations have been carried out, the sets of parameters being defined as follows:

- 5 sections types: HEA280, HEAA220, HEAA300, RHS250/150/6 and SHS180/5;
- 46 calculations for $M_{y,Ed} - M_{z,Ed}$ interaction diagrams (26 for SHS profiles);
- 3 steel grades per section: S235, S275, S355 or S460;
- And 99 additional calculations for welded H-sections.

2.3 Proposed model – Validation and accuracy

As explained in the introduction, the main objective of the Semi-Comp project was the development of adequate design formulae for an enhanced cross-section check of Class 3 sections. Accordingly, the proposed design model had to fulfill several criteria, and amongst them, compatibility with the other formulae of the code (i.e. for compact and slender sections), accuracy, and simplicity.

The design model described hereafter basically relies on a linear transition from the compact (Class 2) to the slender (Class 4) range. Since the proposed formulae had to cover the most complex biaxial bending and compression situation, the model is described in a 3-step procedure, as illustrated on Fig. 5:

- Step 1: determination of the elastic-plastic bending resistance for mono-axial bending ($M_{3,y,Rd}$ and $M_{3,z,Rd}$, see Eq. (3)). A linear interpolation from $M_{pl,Rd}$ to $M_{el,Rd}$ is considered, and a non-dimensional relative "Class 3" slenderness c/t_{ref} is determined so that to vary from 0 at the Class 2-3 border to 1.0 at the Class 3-4 border (see Eqs. (1) and (2));
- Step 2: $M_{Ed} - N_{Ed}$ interaction. The interaction curve for $M_{N,3,y,Rd}$ is linear while it is of parabolic shape for $M_{N,3,z,Rd}$ (see Eq. (4));
- Step 3: biaxial bending interaction between $M_{N,3,y,Rd}$ and $M_{N,3,z,Rd}$. A parabolic interaction was found to be the most appropriate, according to the numerical results (see Eq. (5)).

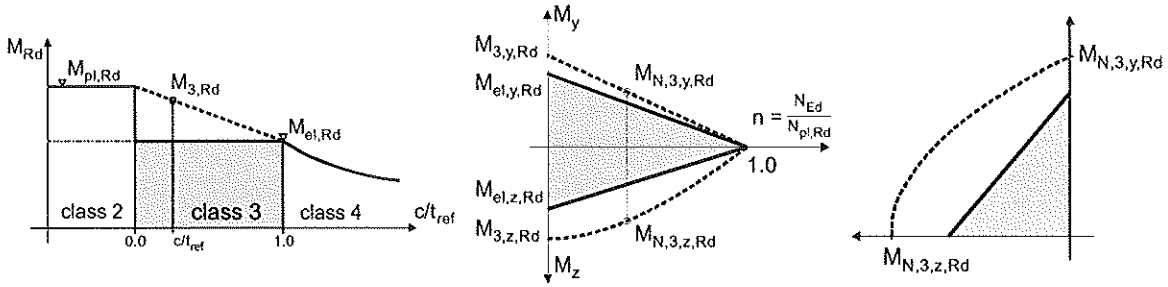

Figure 5: Illustration of the 3-step procedure (grey zones show the Class 3 resistances according to Eurocode 3)

$$\textit{Plate slenderness definition}: \quad \begin{matrix} \beta_{2,y,f}=10\varepsilon & \beta_{2,y,w}=83\varepsilon & \beta_{2,z,f}=10\varepsilon \\ \beta_{3,y,f}=14\varepsilon\beta & \beta_{3,y,w}=124\varepsilon & \beta_{3,z,f}=16\varepsilon \end{matrix} \qquad \varepsilon=\sqrt{235/f_y} \tag{1}$$

$$c/t_{ref,y}=\max\left[\frac{\left(c/t_f-\beta_{2,y,f}\right)}{\left(\beta_{3,y,f}-\beta_{2,y,f}\right)};\frac{\left(c/t_w-\beta_{2,y,w}\right)}{\left(\beta_{3,y,w}-\beta_{2,y,w}\right)}\right] \qquad c/t_{ref,z}=\frac{\left(c/t_f-\beta_{2,z,f}\right)}{\left(\beta_{3,z,f}-\beta_{2,z,f}\right)} \tag{2}$$

Step 1: $$M_{3,i,Rd}=M_{pl,i,Rd}-\left(M_{pl,i,Rd}-M_{el,i,Rd}\right)\cdot c/t_{ref,i} \qquad i=y,z \tag{3}$$

Step 2: $$M_{N,3,y,Rd}=M_{3,y,Rd}\cdot\left(1-n\right) \qquad M_{N,3,z,Rd}=M_{3,z,Rd}\cdot\left(1-n^2\right) \tag{4}$$

Step 3: $$\left[\frac{M_{y,Ed}}{M_{N,red,y,Rd}}\right]^{\alpha}+\left[\frac{M_{z,Ed}}{M_{N,red,z,Rd}}\right]^{\beta}\le 1 \quad where \quad \alpha=2;\ \beta=5n\ge 1 \tag{5}$$

The accuracy of this proposal has been deeply investigated (cf. Semi-Comp 2007). Comparisons with both the experimental tests and the 729 FEM results showed an excellent level of accuracy, and a global average 15% benefit of resistance was observed, in comparison with the actual rules of Eurocode 3. To illustrate these benefits, Fig. 6 depicts the obtained results for the H-shaped sections in the parametric studies, where one clearly notices that the linear interpolation is again fully justified, and that Class 4 cross-sections may also exhibit a certain plastic behavior.

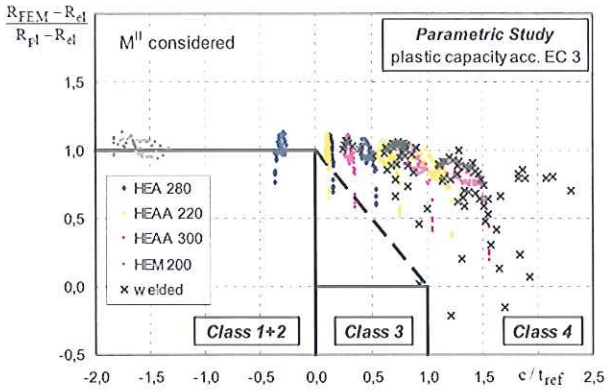

Figure 6: Comparison model vs. FEM results for H-shaped sections

3. Beam-column resistance

3.1 Experimental tests

As explained before, a second series of tests has been conducted on *beam-column members* at the University of Liège. The main aims were to provide information on Class 3 member behavior and to help assessing FEM models.

They basically consisted in mono-axial bending and compression or biaxial bending and compression tests, where bending was applied by means of an eccentrically applied thrust (cf. Fig. 7); the distribution of bending moments was therefore linear for both principal axes.

Cross-section dimensions and member lengths were chosen so that almost all test configurations remain within the semi-compact range for all specimens (see Table 2). Accordingly, four series of 6 tests were performed, with lengths spanning from 3.5m to 4.5m, and nominal steel grades from S275 to S355. Table 2 gives information on the different eccentricities considered and on the obtained experimental failure loads. Additional details on the test setup and specimens measured geometries may be found in final research report (Semi-Comp 2007).

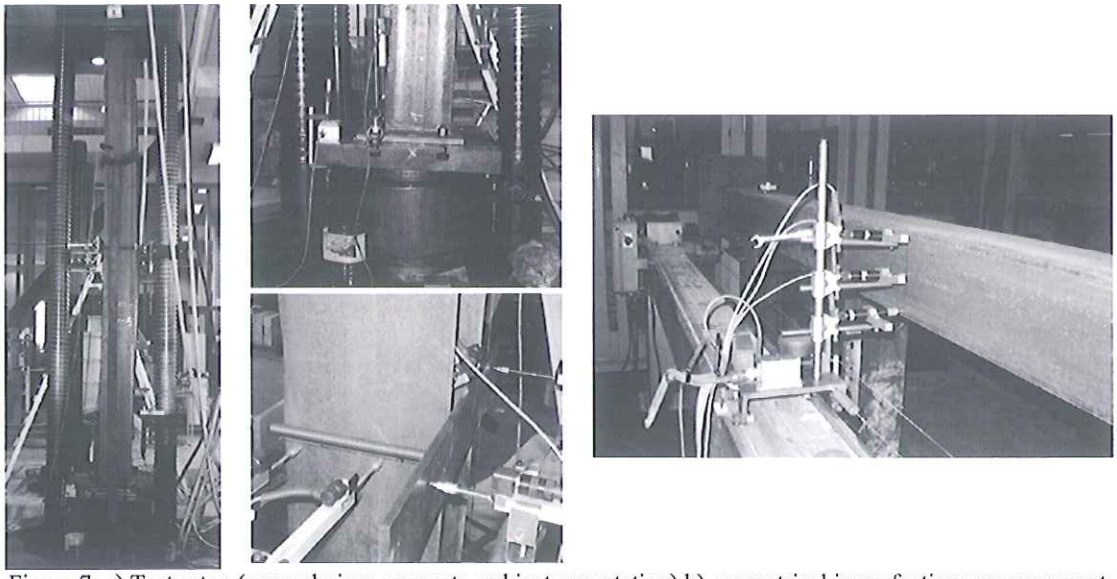
Figure 7: a) Test setup (general view, supports and instrumentation) b) geometrical imperfections measurement

Table 2: Results of tests, FEM simulations and model for *member* resistance

Specimen	L [m]	e_y [mm]	e_z [mm]	P_{test} [kN]	P_{FEM} [kN]	P_{model} [kN]	$\%_{FEM}$ –	$\%_{model}$ –
[1]*H355_1_BU_1 (ψ[2] = 1)*	3.5	85	0	1369	1346	850	1.7	61.0
H355_1_BU_2 (ψ = 0)	3.5	85	0	1636	1605	1059	1.9	54.4
H355_1_BU_3 (ψ = 1)	3.5	0	25	1430	1274	984	12.3	45.3
H355_1_BU_4 (ψ = 0)	3.5	0	25	1650	1512	1107	9.1	49.1
H355_1_BU_5 (ψ = 1)	3.5	85	25	1073	1069	665	0.4	61.5
H355_1_BU_6 (ψ = 0)	3.5	85	25	1393	1380	837	0.9	66.5
[1]*H355_2_BU_1 (ψ = 1)*	4.5	85	0	1180	1139	682	3.6	73.0
H355_2_BU_2 (ψ = 0)	4.5	85	0	1443	1375	864	5.0	67.0
H355_2_BU_3 (ψ = 1)	4.5	0	25	1078	1019	807	5.8	33.6
H355_2_BU_4 (ψ = 0)	4.5	0	25	1281	1186	900	8.0	42.4
H355_2_BU_5 (ψ = 1)	4.5	85	25	896	857	554	4.5	61.8
H355_2_BU_6 (ψ = 0)	4.5	85	25	1161	1066	708	8.9	64.0
[1]*R275_BU_1 (ψ = 1)*	4.0	55	0	404	378	294	7.0	37.2
R275_BU_2 (ψ = 0)	4.0	55	0	451	453	331	-0.4	36.3
R275_BU_3 (ψ = 1)	4.0	0	45	261	239	211	9.2	23.9
R275_BU_4 (ψ = 0)	4.0	0	45	331	296	240	12.0	38.1
R275_BU_5 (ψ = 1)	4.0	55	45	268	225	183	19.3	46.7
R275_BU_6 (ψ = 0)	4.0	55	45	307	282	217	8.8	41.5
[1]*S355_BU_1 (ψ = 1)*	4.0	55	0	563	546	449	3.1	25.4
S355_BU_2 (ψ = 0)	4.0	55	0	656	660	509	-0.6	29.0
S355_BU_3 (ψ = -0.45)	4.0	55	0	708	700	532	1.2	33.1
S355_BU_4 (ψ = 1)	4.0	55	55	460	453	328	1.6	40.3
S355_BU_5 (ψ = 0)	4.0	55	55	600	568	382	5.5	57.1
S355_BU_6 (ψ = -0.45)	4.0	55	55	629	608	419	3.4	50.0

1. "H" stands for HEAA240 section, "R" for RHS200/120/4 and "S" for SHS180/180/5
2. ψ represents the ratio between the applied end moments ($-1 \leq \psi \leq 1$)

Besides this, several "secondary" tests involving usual coupon tests and residual stresses determination were achieved (see Semi-Comp 2007 and Fig. 8). Specific attention was also devoted to the measurements of both *local* and *global* initial geometrical imperfections, in order to provide the necessary information to the FEM models (cf. Fig. 7b).

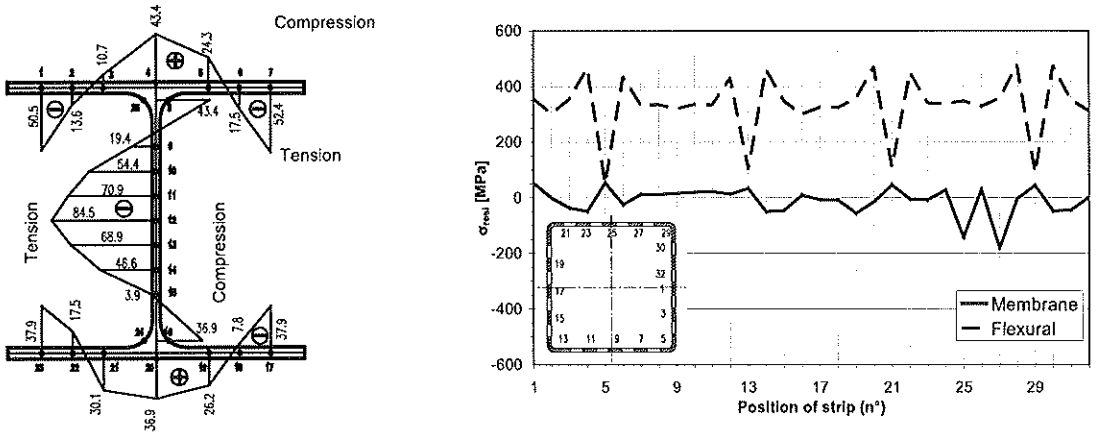

Figure 8: Measured residual stresses a) HEAA240 section b) SHS180/180/5

3.2 FEM modeling and parametric studies

A second set of FEM-shell models for beam-column behavior has been developed at the University of Liège (see Semi-Comp 2007). Like the ones developed at the Technical University

of Graz, they allow for GMNIA computations, account for non-linear σ-ε relationships and residual stresses, and consider both local and global initial geometrical imperfections.
In order to get validated, the models have been compared to the 24 experimental beam-column test results; computations involving the measured properties (dimensions, imperfections...) showed an excellent level of accuracy, as Table 2 and Fig. 9 show.

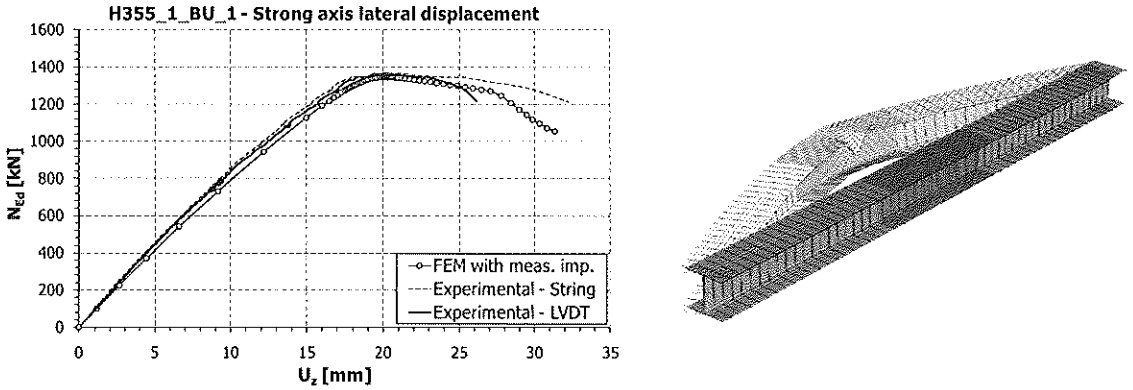

Figure 9: Experimental vs. numerical results for H355_1_BU_1 test

The numerical models being shown to be accurate and appropriate, extensive FEM parametric studies have been performed. The following parameters have been taken into account:

- 4 different cross-section shapes: HEAA220, HEAA300, RHS250/150/6 and SHS180/5;
- 2 values of yield stress: $f_y = 235$ N/mm^2 and $f_y = 355$ N/mm^2;
- 2 primary linear bending moments distributions: $\psi_y = \psi_z = 1$ and $\psi_y = \psi_z = 0$ ($M_{y,Ed}$ and $M_{z,Ed}$ end-moments applied on the same side);
- 2 relative slenderness $\lambda_z = 0.5$ and $\lambda_z = 1.0$;
- 4 different values of relative axial compression $n = N_{Ed} / N_{b,Rd}$: $n = 0$, 0.30, 0.50 and 0.70, where $N_{b,Rd}$ represents the flexural buckling load under pure compression;
- For each fixed values of the previous parameters, 9 combinations of $M_{y,Ed}$ and $M_{z,Ed}$ values have been investigated, so that to allow the determination of the biaxial bending interaction.

In total, 1152 non-linear FEM-shell calculations have been performed, on so-called simply supported members (fork conditions). Due allowance for material imperfections and initial local and global defaults have been made, as explained before.

3.3 Proposed model – Validation and accuracy

According to the project objectives, a design model for *members* has been developed. Further to dealing with member behavior, it also covers cross-sectional behavior, since a section may be seen as a member with vanishing length. The beam-column resistance model has therefore been first developed on the basis of cross-sectional behavior, and then extended to member behavior. Therefore, for what concerns the sole cross-section resistance, it can be seen as an alternative to the model presented in § 2.3.
The basic idea on which this second model relies on again consists in offering an intermediate "elastic-plastic" resistance of the semi-compact cross-section in bending, between pure plastic and pure elastic behavior (see Fig. 1a). In this way, the intermediate distribution of stresses of Fig. 10 is adopted.

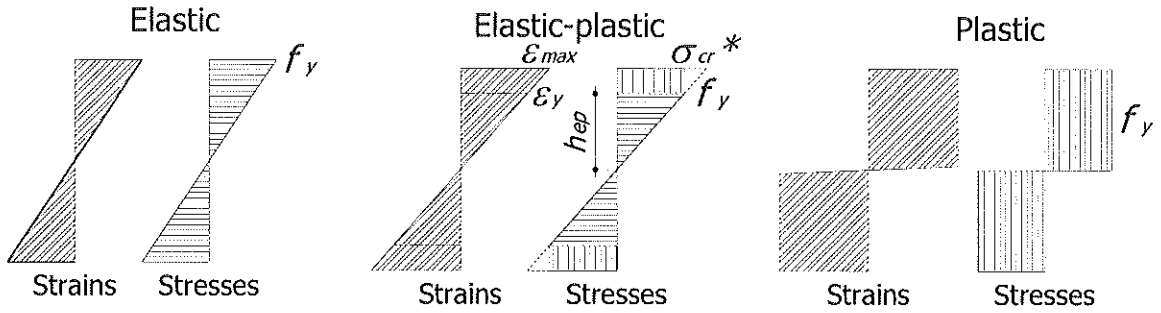

Figure 10: Elastic-plastic distribution of stresses

The total bending resistance then consists of two distinctive contributions (cf. Eq. (6)): a *plastic* contribution $W_{3,pl} f_y$ that corresponds to the yielded fibers of the section, and an *elastic* contribution $W_{3,el} f_y$, arising from the other fibers of the section that have not reached the yield stress yet (fibers within h_{ep}, see Fig. 10).

$$M_{3,Rd} = \left(W_{3,pl} + W_{3,el}\right) f_y \tag{6}$$

Obviously, the key aspect here lies in the correct determination of h_{ep}, that must be so that the cross-section reaches a full plastic resistance at the Class 2 – 3 border (i.e. $h_{ep} \rightarrow 0$), and that the cross-section exhibits its sole elastic resistance at the Class 3 – 4 border (i.e. $h_{ep} = h$, h being the total height of the section). This is achieved in assuming that whenever the stress distribution were still linear beyond f_y, the maximum stress would be equal to σ_{cr}, at a strain level $\varepsilon = \varepsilon_{max} > \varepsilon_y$, ε_y being the maximum elastic strain. The critical plate stress σ_{cr} appears as a convenient stress measure here, since the local (plate) instability effects play the key role.
However, in order to fulfill the continuity aspects at the ends of the Class 3 field, it is necessary to bring "modifications" to the original definition of σ_{cr}. Indeed, in accordance with Fig. 10, σ_{cr} must be so that:

- $\sigma_{cr} = \infty$ at the limit between Class 2 and Class 3;
- $\sigma_{cr} = f_y$ at the limit between Class 3 and Class 4.

In the particular case of a simply supported plate in compression, such a modified σ_{cr}^* writes:

$$\sigma_{cr}^* = 1.616\, E \left(\frac{1}{9.5\, c/t - 323\varepsilon} \right)^2 \tag{7}$$

When σ_{cr}^* is computed, then h_{ep} can be calculated, and so does $M_{3,Rd}$, cf. Eq. (6).
Finally, the design model resorts to the plastic cross-section design checks of Eurocode 3 for combined loading, adequately modified to allow for continuous transitions along the Class 3 range:

$$M_{N,3,i,Rd} = M_{3,i,Rd} \frac{1-n}{1-0.5a\left(1-\dfrac{f_y}{\sigma_{cr}^*}\right)} \leq M_{3,i,Rd} \quad i = y, z \tag{8}$$

$$\left(\frac{M_{y,Ed}}{M_{N,3,y,Rd}}\right)^{\alpha^*}+\left(\frac{M_{z,Ed}}{M_{N,3,z,Rd}}\right)^{\beta^*}\le 1 \quad with \quad \alpha^*=\beta^*=\frac{1.66}{1-1.13n^2}\left(1-\frac{f_y}{\sigma_{cr}^*}\right)+\frac{f_y}{\sigma_{cr}^*}\le 6 \tag{9}$$

The implementation of this cross-section model is straightforward in the Eurocode 3 Method 1 (cf. Maquoi 2001 and Boissonnade 2006) set of beam-column design formulae, cf. Eqs. (12) and (13). Obviously, one must replace $M_{pl,y,Rd}$ and $M_{pl,z,Rd}$ by $M_{3,y,Rd}$ and $M_{3,z,Rd}$ in the different factors, such as for w_y and w_z in the C_{ij} factors for example. In addition, the γ^* and δ^* factors need to be adjusted to:

$$\gamma^*=0.6\sqrt{w_z/w_y}\left(1+\frac{1-0.6\sqrt{w_z/w_y}}{0.6\sqrt{w_z/w_y}}\frac{f_y}{\sigma_{cr}^*}\right) \tag{10}$$

$$\delta^*=0.6\sqrt{w_y/w_z}\left(1+\frac{1-0.6\sqrt{w_y/w_z}}{0.6\sqrt{w_y/w_z}}\frac{f_y}{\sigma_{cr}^*}\right) \tag{11}$$

$$\frac{N_{Ed}}{\chi_y N_{pl,Rd}}+\mu_y\left[\frac{C_{my}M_{z,Ed}}{\left(1-N_{Ed}/N_{cr,y}\right)C_{yy}M_{pl,y,Rd}}\right]+\gamma^*\mu_y\left[\frac{C_{mz}M_{z,Ed}}{\left(1-N_{Ed}/N_{cr,z}\right)C_{yz}M_{pl,z,Rd}}\right]\le 1 \tag{12}$$

$$\frac{N_{Ed}}{\chi_z N_{pl,Rd}}+\delta^*\mu_z\left[\frac{C_{my}M_{z,Ed}}{\left(1-N_{Ed}/N_{cr,y}\right)C_{zy}M_{pl,y,Rd}}\right]+\mu_z\left[\frac{C_{mz}M_{z,Ed}}{\left(1-N_{Ed}/N_{cr,z}\right)C_{zz}M_{pl,z,Rd}}\right]\le 1 \tag{13}$$

Table 3 gives a summary of results on the comparison between numerical and analytical results. The values reported refer to so-called λ-values, which represent the ratio of the $N_{Ed}-M_{y,Ed}-M_{z,Ed}$ loading leading to failure according to the FEM result to the *proportional* $N_{Ed}-M_{y,Ed}-M_{z,Ed}$ loading leading to failure according to the proposed formulae. Consequently, a value higher than unity means safety, while values lower than 1.0 indicates unsafe results. The λ-values also form a good indicator of the level of accuracy of the proposal, a value of 1.10 indicating a 10% resistance reserve. As can be seen, both the mean m and standard deviation s values of the λ-ratios are quite satisfactory, highlighting the good accuracy of the proposal. In comparison with equivalent results provided by Eurocode 3 rules, about 15% better accuracy has been observed.

Table 3: Results of the comparison between FEM results and proposed model for beam-columns

	HEAA220		HEAA300		RHS 250x150x6		SHS 180x5	
	$\psi=1$	$\psi=0$	$\psi=1$	$\psi=0$	$\psi=1$	$\psi=0$	$\psi=1$	$\psi=0$
m	1.141	1.155	1.294	1.348	1.263	1.316	1.275	1.340
s	0.115	0.127	0.271	0.318	0.141	0.183	0.229	0.307
min	0.856	0.900	0.860	0.868	0.916	0.907	0.903	0.917
max	1.434	1.518	2.131	2.572	1.552	1.756	1.820	2.092
Σtests	144	144	144	144	144	144	144	144

Fig. 10a also further illustrates the ability of the proposed model to lead to intermediate results between full *plastic* behavior and pure *elastic* behavior. It clearly shows that in the particular case of the figure, it would appear unnecessarily conservative to restrict the resistance of such members to their sole elastic carrying capacity. The tendency of exhibiting a certain level of plastic behavior has been generally observed on the cases studied, even in situations where the

cross-section is classified as Class 4, as Fig. 10b shows. Such results are especially responsible for the high λ-ratios reported in Table 3.

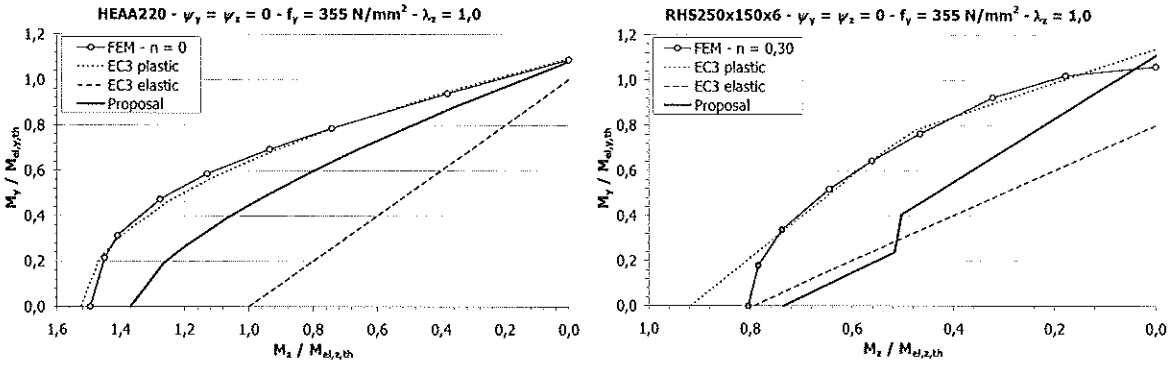

Figure 11: a) Illustration of an intermediate elastic-plastic behavior b) Situation where plastic reserve is observed while cross-section is Class 4 or nearly (left first 3 points are Class 4)

4. Conclusions

Present research works were focused on the specific behavior of semi-compact "Class 3" sections and profiles; the purpose was here to propose simple design rules providing smooth resistance transitions within the Class 3 range. Based on the results of more than 80 tests and 2500 FEM simulations, the proposed mechanical models, covering both section and member behavior, have been shown to lead to an excellent level of accuracy as well as to offer full continuities between cross-section classes and with all other design formulae of the code; these models may be further used in design practice and incorporated in the coming version of the European standard, i.e. Eurocode 3.

Acknowledgments

The Research Fund for Coal and Steel (RFCS), by means of research project "Semi-Comp" n°RFS-CR-04044, is gratefully acknowledged.

References

Boissonnade N., Greiner R. Jaspart J.P., Lindner J. (2006). "Rules for Member Stability in EN 1993–1–1; Background documentation and design guidelines". Eds. Mem Martins, Portugal, ECCS – ISBN 92-9147-000-84, Vol. 119.

Boissonnade N., Jaspart J.P., Oerder R., Weynand K. (2008). "A new Design Model for the Resistance of Steel Semi-compact Cross-sections", *Proceedings of the 5th European Conference on Steel Structures*, Eurosteel 2008, Graz, September 3-5.

CEN (Comité Européen de Normalisation). (2005). "Eurocode 3: Design of Steel Structures, Part 1–1: General Rules and Rules for Buildings (EN 1993 1–1)", Brussels.

Kettler, M. (2008). "Elastic-Plastic Cross-Sectional Resistance of Semi-Compact H- and Hollow Sections." *Dissertation*, Institut für Stahlbau und Flächentragwerke, TU Graz.

Lechner, A. (2005). "Plastic Capacity of Semi-Compact Cross-Sections." *Dissertation*, Institut für Stahlbau und Flächentragwerke, TU Graz.

Maquoi, R., Boissonnade, N., Muzeau, J.P., Jaspart, J.P., Villette, M. (2001). "The Interaction Formulae for Beam-Columns: A New Step of a Yet Long Story", *Proceedings of the 2001 SSRC Annual Technical Session & Meeting*, Fort Lauderdale, May 9, 63-88.

"Plastic member capacity of semi-compact steel sections – a more economic design (Semi-Comp)" (2007). *Final report (01/01/06 – 30/06/07)* – RFCS – Steel RTD (Contract RFS-CR-04044).